IEEE Access
Multidisciplinary | Rapid Review | Open Access Journal

Received 20 June 2022, accepted 5 July 2022, date of publication 13 July 2022, date of current version 18 July 2022.

Digital Object Identifier 10.1109/ACCESS.2022.3190624

RESEARCH ARTICLE

Fundamental Limits on the Uplink Performance of the Dynamic-Ordered SIC Receiver

LUCA LUSVARGHI, (Graduate Student Member, IEEE), AND MARIA LUISA MERANI, (Senior Member, IEEE)
Department of Engineering "Enzo Ferrari," University of Modena and Reggio Emilia, 41125 Modena, Italy
Consorzio Nazionale Interuniversitario per le Telecomunicazioni (CNIT), 43124 Parma, Italy

Corresponding author: Luca Lusvarghi (luca.lusvarghi5@unimore.it)

This work was supported by the Department of Engineering "Enzo Ferrari," University of Modena and Reggio Emilia, under Grant FAR 2022.

ABSTRACT Due to the rapid and widespread growth of the Internet-of-Things (IoT) paradigm, present days witness an exponential increase in the number of connected devices. In this regard, the orthogonal transmission techniques featured by conventional 4G and 5G systems can only support a limited number of simultaneously active users, due to their low spectral efficiency and poorly flexible resource allocation. To overcome such limitations, the 6G framework will include novel Next Generation Multiple Access (NGMA) solutions that will efficiently and flexibly connect a significantly larger number of devices over the same portion of spectrum. Under the NGMA umbrella, the Power-Domain Non-Orthogonal Multiple Access (PD-NOMA) technology is able to accommodate multiple users on the same frequencies by carefully assigning different power levels to the active users and employing Successive Interference Cancellation (SIC) receivers. In this work, we put forth a novel analytical approach to evaluate the performance that PD-NOMA achieves on the uplink of a single cell when a dynamic-ordered SIC receiver is considered. With respect to other existing works, the fundamental limits on the system performance are assessed analytically for an arbitrary number n of simultaneously transmitting users, and both the case of Rayleigh and lognormal-shadowed Rayleigh fading are examined. The closed-form expressions presented in this work, whose correctness and excellent accuracy are validated through Monte Carlo simulations, disclose the impact of lognormal shadowing and an increasingly larger number of active users on the PD-NOMA performance.

INDEX TERMS Non-orthogonal multiple access, power-domain NOMA, NOMA, outage probability, dynamic-ordered SIC, order statistics.

I. INTRODUCTION

Scanning the 5G and beyond horizon, wireless connectivity appears as one of the key enabling technologies for future Internet of Things (IoT). According to Cisco [1], the number of connected devices is yet growing at an extraordinary pace and is expected to reach a total of 29.3 billion devices by 2023, with IoT connections accounting for half of the total. Such a massive demand for Internet connectivity, along with the heterogeneous set of performance requirements which characterizes IoT devices [2], transcends the capabilities of fourth generation (4G) and fifth generation (5G) systems. Relying on orthogonal transmission techniques, these systems can only support a limited number of simultaneously active users, and advocate for the design of new connectivity solutions. In this direction, sixth generation (6G) cellular systems will feature novel Next Generation Multiple Access (NGMA) schemes able to guarantee massive connectivity, improved energy efficiency, and lower latency.

Under the NGMA umbrella, Non-Orthogonal Multiple Access (NOMA) techniques are expected to play a pivotal role in the support of unprecedented connectivity capabilities [3]. The key idea behind NOMA, i.e., serving multiple users over the same radio spectrum, has been widely investigated over the last years, breeding an abundant body of scientific literature and the proposal of many distinct NOMA

The associate editor coordinating the review of this manuscript and approving it for publication was Khaled Rabie.

approaches. Among them, there appear Power-Domain (PD)-NOMA, Sparse Code (SC)-NOMA, and Resource Spread (RS)-NOMA, to name a few examples. As a result, the risk that every NOMA bibliography incurs is to forget or inadvertently miss some relevant works among the multitude of published papers. For this reason, the surveys reported in [4]–[7] are mentioned in this Introduction together with [8] and [9], which provide a comprehensive comparison between NOMA techniques and alternative NGMA schemes such as Multi-User Multiple-Input Multiple-Output (MU-MIMO), and Rate-Splitting Multiple Access (RSMA).

Specifically, this work concentrates on PD-NOMA. PD-NOMA multiplexes multiple users on the same radio resources by assigning them different transmit power levels, and it can be employed in both downlink and uplink communications. At the receiver side, the superimposed signals are separately decoded using Successive Interference Cancellation (SIC). Confining the attention to PD-NOMA, simply referred to as NOMA in the rest of this paper, its behavior has been assessed in numerous studies. For example, the authors in [10] showed the potential of NOMA in mitigating traffic congestion and reducing latency when 5G Vehicle-to-Everything (V2X) downlink transmissions are considered. The performance of random access uplink NOMA was evaluated in [11] from a system-level perspective, i.e., in terms of throughput and access delay, whereas an analytical framework for the modeling and the analysis of large-scale uplink and downlink NOMA systems has been proposed in [12], [13]. The studies in [14], [15] highlighted the strengths and the limitations which characterize a typical SIC-based decoding process in uplink and downlink NOMA communications, and put forth the design of a new hybrid SIC receiver. Moreover, it is worth recalling the contributions in [16] and [17]. In the former, the performance of uplink NOMA, paired with a dedicated power control scheme, was analyzed in terms of outage probability and achievable data rate. In the latter, the authors proposed a novel uplink NOMA scheme able to achieve higher spectral efficiency and lower receiver complexity with respect to conventional techniques. Stemming from [16], [18] focused on the optimization of the power allocation strategy. Differently from the contributions mentioned so far, where a fixed decoding order SIC receiver was considered, the authors of [19] and [20] analyzed NOMA systems employing dynamic-ordered SIC receivers. The dynamic-ordered SIC receiver adaptively varies the decoding order on the basis of the instantaneously received signals power. These works determined closed-form expressions of the outage probability for the case of three users, without however providing a systematic analysis. In [21], the Signal-to-Interference Ratio (SIR) coverage probability of uplink NOMA was evaluated, comparing the performance of two SIC receivers; namely, the dynamic-ordered SIC receiver was confronted against a SIC receiver that ranks and decodes the users' signals on the basis of their mean received powers.

It is worth pointing out that all the previous investigations were performed in the exclusive presence of Rayleigh fading, an assumption that greatly simplifies the study. In this regard, the work in [22] introduced the hypothesis of generalized fading channels encompassing statistics such as Rayleigh, Rice, and Nakagami, and considered a fixed decoding order SIC. Due to the complex nature of the analysis, the authors exclusively considered the circumstance of two superimposed users for mathematical tractability. In [23], the channel model was the generalized α-μ fading and, also in this work, the SIC decoding order was fixed; here too, the analysis was limited to the circumstance of two or at the most three simultaneously active users.

In this work, we analytically assess the performance of a Single-Input Single-Output (SISO) uplink NOMA system when a dynamic-ordered SIC receiver is considered. The assumption of only two or three superimposed signals usually found in literature is removed to disclose the fundamental limits on the achievable performance of the receiver. Furthermore, the analysis in the presence of Rayleigh fading is extended by the investigation of the combined effects of fading and lognormal shadowing. To characterize system behavior, the outage probabilities $P_{out}^{(j)}$, $j = 1, 2, \ldots, n$, are determined, the generic $P_{out}^{(j)}$ being defined as the probability that the receiver fails to decode the j-th strongest signal and therefore cannot recover the remaining $n - j$ weaker signals. With respect to the state-of-the-art, this work offers several novel contributions:

- a general method to analytically evaluate the outage probabilities is provided, based on the unique properties of the joint probability density function of the ordered received powers, as the latter are dependent, non identically distributed random variables. The approach can be profitably employed for any number n of simultaneously received signals;
- when Rayleigh fading is considered, the exact analytical expression of $P_{out}^{(1)}$, the probability that the strongest signal cannot be decoded and that the SIC receiver fails to recover any of the simultaneous signals, is provided for an arbitrary value of n. When the first strongest signal can be decoded, a closed-form approximation of $P_{out}^{(j)}$, $j \geq 2$, is also put forth in order to characterize the performance of the remaining $n - 1$ active users;
- when the signals are affected by Rayleigh-lognormal shadowed fading, an approximation of the outage probability $P_{out}^{(j)}$, $j \geq 1$, is offered, demonstrating that it achieves an excellent accuracy, again for an arbitrary n;
- the proposed approximations show that, j being fixed, $P_{out}^{(j)}$, $j \geq 2$, can be recursively evaluated as a function of the probabilities $P_{out}^{(1)}$ obtained in the presence of n, $n - 1, \ldots, n - j + 1$ simultaneously active users.

Overall, the analysis discloses the limits that the dynamic-ordered SIC receiver faces for an increasing number of superimposed signals, when an uplink NOMA system is considered. Furthermore, it reveals that lognormal shadowing is responsible for a non-negligible performance worsening, with respect to the circumstance where Rayleigh fading only

is considered. The deterioration is quantified for different values of σ_L, the standard deviation of the slow, lognormal fading in dB.

The remainder of the paper is organized as follows. Section II introduces the system model, it illustrates the analysis and it puts forth the approximations to the outage probabilities experienced on the uplink. Section III specializes the study to the cases of Rayleigh and Rayleigh-lognormal shadowed fading. Section IV provides several numerical results that validate the approach and Section V draws the conclusions.

II. PERFORMANCE ANALYSIS

A. SYSTEM MODEL AND PERFORMANCE METRIC EVALUATION

The current work focuses on the uplink communications in a cellular system. Power-domain NOMA is considered and the reference scenario features n User Equipments (UEs) that transmit to a central-located base station on the same radio spectrum. Let $p_{t,i}$ denote the transmission power of the i-th UE and h_i the envelope of the channel between such UE and the base station. Let

$$X_i = p_{t,i}|h_i|^2 \qquad i = 1, 2, \ldots, n \tag{1}$$

denote the instantaneously received power at the base station from the i-th UE. Further assume that every UE experiences independent channel conditions while transmitting to the base station; it follows that h_i and h_j are independent random variables, $\forall\ i$ and j, $i \neq j$, and so are X_i and X_j. Moreover, assume that the signal recovery is performed using a dynamic-ordered SIC receiver. This choice implies that: (i) the instantaneously received signal powers from the UEs are first sorted in descending order at the base station; (ii) the receiver attempts to decode the signals in accordance to the same sequence.

Indicate by $\mathcal{S}_{\mathcal{N}}$ the set of the $n!$ permutations of $N = \{1, 2, \ldots, n\}$ and by $R = \{r_1, r_2, \ldots, r_n\}$, $R \in \mathcal{S}_{\mathcal{N}}$, the permutation that corresponds to the descending order of the instantaneously received powers. It follows that

$$p_{t,r_1}|h_{r_1}|^2 \geq p_{t,r_2}|h_{r_2}|^2 \geq \ldots \geq p_{t,r_n}|h_{r_n}|^2. \tag{2}$$

where p_{t,r_1} is the transmitted power of the UE that exhibits the highest received power, p_{t,r_2} the transmitted power of the UE that exhibits the second highest received power, and so forth.

Next, introduce the random variables

$$X_{(i)} = p_{t,r_i}|h_{r_i}|^2 \qquad i = 1, 2, \ldots, n \tag{3}$$

and observe that the $X_{(i)}$s are no longer independent. Rather, owing to (2) they constitute an order statistics; for the notation employed, $X_{(1)}$ is the largest order statistic, $X_{(n)}$ is the smallest.

The receiver first attempts to decode the strongest signal. If the decoding process is successful, the receiver removes the first strongest signal and then proceeds to decode the second strongest. For the base station to decode the message from the j-th strongest user $\mathrm{UE}_{(j)}$, the $j-1$ received signals with the strongest power have to be successfully recovered and removed first.

Recalling Shannon's capacity theorem, the achievable data rate of $\mathrm{UE}_{(j)}$ is

$$R_{(j)} = \log_2\left(1 + \frac{X_{(j)}}{\sum_{i=j+1}^{n} X_{(i)} + \sigma^2}\right) \quad \text{bits/s/Hz}, \tag{4}$$

for $j = 1, 2, \ldots, n-1$, where σ^2 is the noise power, and

$$R_{(n)} = \log_2\left(1 + \frac{X_{(n)}}{\sigma^2}\right) \quad \text{bits/s/Hz} \tag{5}$$

for the last user $\mathrm{UE}_{(n)}$, whose received power is the weakest.

Denote by $\hat{R}_{(j)}$ the target data rate of $\mathrm{UE}_{(j)}$ and define the outage probability $P_{out}^{(j)}, j = 1, 2, \ldots, n$, as the probability that the SIC receiver can successfully recover the first strongest signal, the second strongest, up to the $j-1$, but it fails to decode the j-th strongest and all the subsequent signals. Analytically,

$$P_{out}^{(j)} = 1 - P\{R_{(j)} \geq \hat{R}_{(j)}\}. \tag{6}$$

If we indicate by $\mathcal{E}_k, k = 1, 2, \ldots, n-1$, the random event identified by the condition

$$\frac{X_{(k)}}{\sum_{i=k+1}^{n} X_{(i)} + \sigma^2} \geq \hat{\gamma}_k \tag{7}$$

where

$$\hat{\gamma}_k = 2^{\hat{R}_{(k)}} - 1, \quad k = 1, 2, \ldots, n, \tag{8}$$

and by $\mathcal{E}_n$ the event in which the condition

$$\frac{X_{(n)}}{\sigma^2} \geq \hat{\gamma}_n \tag{9}$$

holds, then (6) is equivalently re-written as

$$P_{out}^{(j)} = 1 - P\left\{\cap_{k=1}^{j}\mathcal{E}_k\right\}, \quad j = 1, 2, \ldots, n, \tag{10}$$

where it is observed that the random events $\mathcal{E}_1, \mathcal{E}_1, \ldots, \mathcal{E}_n$ are statistically dependent.

Indicate by $f_{joint_n}(x_{(1)}, x_{(2)}, \ldots, x_{(n)})$ the joint probability density function (pdf) of the ordered set of random variables $X_{(i)}$, $i = 1, 2, \ldots, n$, and by $\mathcal{D}_j$ the region of the $X_{(1)}$, $X_{(2)}, \ldots, X_{(n)}$ space identified by the conditions:

$$\mathcal{D}_j = \begin{cases} X_{(1)} \geq \hat{\gamma}_1 \cdot (\sum_{i=2}^{n} X_{(i)} + \sigma^2) \\ X_{(2)} \geq \hat{\gamma}_2 \cdot (\sum_{i=3}^{n} X_{(i)} + \sigma^2) \\ \vdots \\ X_{(j)} \geq \hat{\gamma}_j \cdot (\sum_{i=j+1}^{n} X_{(i)} + \sigma^2) \\ 0 \leq X_{(n)} \leq X_{(n-1)} \leq \cdots \leq X_{(2)} \leq X_{(1)}. \end{cases} \tag{11}$$

It follows that $P_{out}^{(j)}, j = 1, 2, \ldots, n$, is determined solving the integral

$$P_{out}^{(j)} = 1 - \int \cdots \int_{\mathcal{D}_j} f_{joint_n}(x_{(1)}, x_{(2)}, \ldots, x_{(n-1)}, x_{(n)}) \times dx_{(n)}dx_{(n-1)} \ldots dx_{(2)}dx_{(1)}. \tag{12}$$

Among the different outage probabilities $P_{out}^{(j)}$, observe that $P_{out}^{(1)}$ deserves a special place, as it coincides with the probability that the strongest signal cannot be correctly recovered; in this circumstance, not even one, out of the n simultaneous transmissions, can be successfully decoded and power-domain NOMA fails. Indeed, the inequality $X_{(1)} \geq \hat{\gamma_1} \cdot (\sum_{i=2}^{n} X_{(i)} + \sigma^2)$ identifying the outage domain $\mathcal{D}_1$ represents the necessary condition for the SIC decoding process to begin. Equivalently stated, $P_{out}^{(1)}$ gives the probability that the adoption of power-based NOMA turns out detrimental, as not even the best signal is correctly decoded.

When evaluating $P_{out}^{(j)}$, the first non-trivial problem at hand is to determine $f_{joint_n}(x_{(1)}, x_{(2)}, \ldots, x_{(n)})$. In this respect, let $f_i(x_i)$ be the pdf of the *unordered* random variable X_i, $i = 1, 2, \ldots, n$, defined in (1), whose pdf is available once the pdf of h_i is known, as $p_{t,i}$ is a constant, and define F_n as the following $n \times n$ matrix

$$F_n = \begin{bmatrix} f_1(x_{(1)}) & f_2(x_{(1)}) & \ldots & f_n(x_{(1)}) \\ f_1(x_{(2)}) & f_2(x_{(2)}) & \ldots & f_n(x_{(2)}) \\ \vdots & \vdots & \ddots & \vdots \\ f_1(x_{(n)}) & f_2(x_{(n)}) & \ldots & f_n(x_{(n)}) \end{bmatrix} \tag{13}$$

where $f_j(x_{(i)})$ denotes the pdf of the unordered random variable X_j, $j = 1, 2, \ldots, n$, when the function argument is the random sample $x_{(i)}$ of the ordered random variable $X_{(i)}$. For the purpose of what follows, recall that the permanent of a square matrix A, written as $\overset{+}{|}A\overset{+}{|}$, is defined like the determinant, except that all signs are positive. For an arbitrary n, it can be demonstrated that the joint pdf $f_{joint_n}(x_{(1)}, x_{(2)}, \ldots, x_{(n)})$ of the ordered statistics $X_{(1)}, X_{(2)}, \ldots, X_{(n)}$ is

$$f_{joint_n}(x_{(1)}, x_{(2)}, \ldots, x_{(n)}) = \overset{+}{|}F_n\overset{+}{|}, \tag{14}$$

where F_n is given by (13). Last result is substantiated by the reasoning in [24], where the arguments of [25] are extended to prove the formulation in (14) with the use of permanents.

At first sight, (14) gives the impression that evaluating the integral in (12) might be quite cumbersome for an arbitrary value of n. However, the joint pdf obeys a highly peculiar structure, that allows a more convenient rewriting of it in the following terms: let $S_i = \{i_1, i_2, \ldots, i_n\}$ denote the generic permutation of $N = \{1, 2, \ldots, n\}$ in $\mathcal{S}_\mathcal{N}$, where we recall that the latter symbol indicates the set of all possible permutations. It follows that $f_{joint_n}(x_{(1)}, x_{(2)}, \ldots, x_{(n)})$ can be equivalently written as

$$f_{joint_n}(x_{(1)}, x_{(2)}, \ldots, x_{(n)}) = \sum_{S_i \in \mathcal{S}_\mathcal{N}} f_1(x_{(i_1)}) f_2(x_{(i_2)}) \ldots f_n(x_{(i_n)}). \tag{15}$$

Last expression highlights that the joint pdf exhibits the presence of $n!$ terms, wherein the permutations of the arguments of the $f_1(\cdot), f_2(\cdot), \ldots, f_n(\cdot)$ pdfs appear. Replacing (15) in (12) leads to

$$P_{out}^{(j)} = 1 - \int \cdots \int_{\mathcal{D}_j} \sum_{S_i \in \mathcal{S}_\mathcal{N}} f_1(x_{(i_1)}) f_2(x_{(i_2)}) \ldots f_n(x_{(i_n)}) \times dx_{(n)} dx_{(n-1)} \ldots dx_{(2)} dx_{(1)} \tag{16}$$

and denoting by I_{S_i} the result of the integral

$$I_{S_i} = \int \cdots \int_{\mathcal{D}_j} g_{i_1 i_2 \ldots i_n}(x_{(1)}, x_{(2)}, \ldots, x_{(n)})\, dx_{(n)} \ldots dx_{(1)}, \tag{17}$$

where

$$g_{i_1 i_2 \ldots i_n}(x_{(1)}, x_{(2)}, \ldots, x_{(n)}) = f_1(x_{(i_1)}) f_2(x_{(i_2)}) \cdot \ldots \cdot f_n(x_{(i_n)}), \tag{18}$$

then $P_{out}^{(j)}$ can be rewritten as:

$$P_{out}^{(j)} = 1 - \sum_{S_i \in \mathcal{S}_\mathcal{N}} I_{S_i}, \quad \forall j, j = 1, 2, \ldots, n. \tag{19}$$

Luckily, the random variables $X_1, X_2, \ldots, X_n$ obey the same statistical description, although with different mean values. It follows that it is not necessary to compute every single I_{S_i} term in (19). Rather, the *n-th* fold integral in (17) has to be solved only once, for a specific S_i. For instance, I_{S_1} can be determined, $S_1 = \{1, 2, \ldots, n\}$. Then, all the remaining I_{S_i} terms are obtained through the proper permutation of the $f_i(\cdot)$'s arguments $x_{(i_k)}$, $k = 1, 2, \ldots, n$ in (18). This significantly reduces $P_{out}^{(j)}$ computational complexity in n regardless of the channel envelope statistics, i.e., no matter what pdf the random variables h_i, $i = 1, 2, \ldots, n$, obey to.

Once $P_{out}^{(j)}$ has been obtained, the sum data rate that power-domain NOMA achieves is evaluated as:

$$R_{NOMA} = \sum_{j=1}^{n} \hat{R}_{(j)} \cdot \left(1 - P_{out}^{(j)}\right). \tag{20}$$

B. $P_{out}^{(j)}$ APPROXIMATION FOR $j \geq 2$

The previous development highlighted how to reduce the complexity that hinders behind the exact analytical evaluation of the outage probability $P_{out}^{(j)}, j = 1, 2, \ldots, n$. The approach turns out particularly effective when evaluating $P_{out}^{(1)}$. When $j \geq 2$, the difficulty in evaluating $P_{out}^{(j)}$ has also to be ascribed to an increasing complexity of the integration domain $\mathcal{D}_j$ in (11), as well as to the dependency among the events $\mathcal{E}_1, \mathcal{E}_2, \ldots, \mathcal{E}_j$. To alleviate the computational burden, this subsection explores the following approximation to $P_{out}^{(j)}, j \geq 2$:

$$P_{out}^{(j)} \approx 1 - \prod_{k=1}^{j} P\{\mathcal{E}_k\}, \quad j \geq 2, \tag{21}$$

that holds under the assumption that the random events $\mathcal{E}_k$, $k = 1, 2, \ldots, n$, be weakly dependent. To the authors' knowledge, there is no general result in the vast literature on ordered statistics that come to help in corroborating the above approximation. It has however been employed before,

e.g., in [16], [19], [20]. In this work, we follow the same approach, and *a posteriori* demonstrate that it holds.

Let us begin considering the case of $n = 2$ UEs. In addition to $P_{out}^{(1)}$, only $P_{out}^{(2)}$, the probability that the receiver fails to decode the second strongest signal, has to be determined. If we recall (7) and (9), $P_{out}^{(2)}$ specializes to

$$P_{out}^{(2)} \approx 1 - P\left\{\frac{X_{(1)}}{X_{(2)} + \sigma^2} \geq \hat{\gamma}_1\right\} \cdot P\left\{\frac{X_{(2)}}{\sigma^2} \geq \hat{\gamma}_2\right\}; \quad (22)$$

it is easy to recognize that the first term in the product on the right-hand side of (22) coincides with $1 - P_{out}^{(1)}$. Moreover, indicating by $G_{(2)}(\cdot)$ the Cumulative Distribution Function (CDF) of the random variable $X_{(2)}$, (22) is equivalently re-written as

$$P_{out}^{(2)} \approx 1 - \left(1 - P_{out}^{(1)}\right) \cdot \left(1 - G_{(2)}(\hat{\gamma}_2\sigma^2)\right). \quad (23)$$

With no loss in generality, let the unordered random variables X_i, $i = 1, 2, \ldots, n$, be numbered in accordance to the descending order of their mean received powers, so that $\overline{X}_1 > \overline{X}_2 > \ldots > \overline{X}_n$. Moreover, let us assume that the random variable δ_i measuring the spacing between X_i and X_{i-1}, $\delta_i = |X_i - X_{i-1}|$, $i = 2, \ldots, n$, takes on large values with probability close to 1. In the scenarios where uplink NOMA is profitably employed, such approximation is verified, i.e., the spacing δ_i is sufficiently wide; as a matter of fact, this is the condition that allows to better discriminate among simultaneously received signals. Given this assumption holds, observe that it is possible to leverage upon a further approximation, namely, $G_{(2)}(\cdot)$ that appears in (23) is replaced by $G_2(\cdot)$, the CDF of the unordered random variable X_2. This leads to

$$P_{out}^{(2)} \approx 1 - \left(1 - P_{out}^{(1)}\right) \cdot \left(1 - G_2(\hat{\gamma}_2\sigma^2)\right) \quad (24)$$

that represents the final, approximated $P_{out}^{(2)}$ expression when $n = 2$.

When $n = 3$ UEs are present, $P_{out}^{(2)}$ and also $P_{out}^{(3)}$ have to be determined. The probability $P_{out}^{(2)}$ modifies in

$$P_{out}^{(2)} \approx 1 - P\left\{\frac{X_{(1)}}{X_{(2)} + X_{(3)} + \sigma^2} \geq \hat{\gamma}_1\right\} \cdot P\left\{\frac{X_{(2)}}{X_{(3)} + \sigma^2} \geq \hat{\gamma}_2\right\}, \quad (25)$$

and denoting by $P_{out_{2,3}}^{(1)}$ the probability $P\left\{\frac{X_{(2)}}{X_{(3)}+\sigma^2} \geq \hat{\gamma}_2\right\}$, then $P_{out}^{(2)}$ is expressed as

$$P_{out}^{(2)} \approx 1 - \left(1 - P_{out}^{(1)}\right) \cdot \left(1 - P_{out_{2,3}}^{(1)}\right) \quad (26)$$

As regards $P_{out}^{(3)}$, the same approximation leveraged in (24) leads to

$$P_{out}^{(3)} \approx 1 - \left(1 - P_{out}^{(1)}\right) \cdot \left(1 - P_{out_{2,3}}^{(1)}\right) \cdot \left(1 - G_3(\hat{\gamma}_3\sigma^2)\right), \quad (27)$$

$G_3(\cdot)$ being the CDF of the unordered random variable X_3.

When an arbitrary number n of UEs is considered, the approximated expression of $P_{out}^{(j)}$, $j \leq n$, is provided by (28), as shown at the bottom of the page, where $P_{out_{h+1,h+2,\ldots,n}}^{(1)}$ is defined as $P\left\{\frac{X_{(h+1)}}{X_{(h+2)}+\ldots+X_{(n)}} \leq \hat{\gamma}_{h+1}\right\}$, and $G_n(\cdot)$ is the CDF of the n-th random variable X_n, i.e., the CDF of the power received from the most distant user from the base station.

Last expression is illuminating, as it reveals that: (i) the outage probability $P_{out}^{(j)}$, $j \geq 2$, depends on $P_{out}^{(1)}$, the probability that NOMA fails in the presence of the same number of users; (ii) moreover, $P_{out}^{(j)}$ can be readily computed, given the expression of $P_{out}^{(1)}$ in the presence of n, $n-1, \ldots, n-j+1$ users is known. Finally, observe that the expressions we have obtained can be employed when different fading conditions are examined.

The Numerical Results highlight that it is possible to rely upon the proposed approximation of $P_{out}^{(j)}$, $j \geq 2$, in several meaningful settings. To the authors' knowledge, there is however no means to conclude whether (28) provides an upper or lower bound to the outage.

When Rayleigh fading is considered, next Section reports the exact analytical expression of $P_{out}^{(1)}$ derived in the Appendix, and the closed-form approximation of $P_{out}^{(j)}$, $j \geq 2$, for an arbitrary number of simultaneously transmitting UEs. When shadowing is also introduced, the closed-form approximation of $P_{out}^{(j)}$ is provided for $j \geq 1$.

III. FADING MODELS

A. RAYLEIGH FADING

When the presence of Rayleigh fading is assumed, the probability density function (pdf) of the received signal power X_i is exponential:

$$f_i(x_i) = \frac{1}{\overline{X}_i} \exp\left(\frac{-x_i}{\overline{X}_i}\right) \quad (29)$$

with mean $\overline{X}_i$,

$$\overline{X}_i = p_{t,i} \cdot k_p D_i^{-\alpha}, \quad (30)$$

k_p being a constant that depends on the operating frequency and D_i the distance between UE$_i$ and the base station.

$$P_{out}^{(j)} \approx \begin{cases} 1 - \left(1 - P_{out}^{(1)}\right) \cdot \prod_{h=1}^{j-1} \left(1 - P_{out_{h+1,h+2,\ldots,n}}^{(1)}\right) & j < n \\ 1 - \left(1 - P_{out}^{(1)}\right) \cdot \prod_{h=1}^{n-1} \left(1 - P_{out_{h+1,h+2,\ldots,n}}^{(1)}\right) \cdot \left(1 - G_n(\hat{\gamma}_n\sigma^2)\right) & j = n \end{cases} \quad (28)$$

In Appendix A, it is proved that when $\hat{\gamma}_1 \geq 1$, for an arbitrary number of users n, $P_{out}^{(1)}$ obeys the expression:

$$P_{out}^{(1)} = 1 - \sum_{k=1}^{n} \frac{\exp\left(\frac{-\hat{\gamma}_1 \sigma^2}{\overline{X}_k}\right)}{\prod_{\substack{i=1 \\ i \neq k}}^{n} \left(1 + \frac{\overline{X}_i}{\overline{X}_k} \hat{\gamma}_1\right)} \tag{31}$$

that reveals what limits NOMA faces, if the number n of simultaneously active users is increased from 2 to higher values.

In turn, taking advantage of (31), the fading-independent approximation of $P_{out}^{(j)}$ provided by (28), $j \geq 2$, specializes to (32), as shown at the bottom of the page.

The constraint on $\hat{\gamma}_1$ deserves a careful remark: it is the authors' belief that it does not represent a limiting factor, rather, a fairly widespread requirement in upcoming settings. As an example, high-end industrial IoT use cases are expected to require conspicuous data rates, exceeding the system available bandwidth, to support video-assisted services ranging from process monitoring to augmented video-reality [2].

B. RAYLEIGH-LOGNORMAL SHADOWED FADING

When the envelope of the received signal is subject to both Rayleigh fading and lognormal shadowing, the X_i pdf is

$$f_i(x_i) = \int_0^{+\infty} \frac{1}{\overline{x}} \exp\left(\frac{-x_i}{\overline{x}}\right) \frac{1}{\sqrt{2\pi}\frac{\sigma_L}{h}\overline{x}} \times \exp\left(-\frac{(\ln(\overline{x}) - \mu_i)^2}{\frac{2\sigma_L^2}{h^2}}\right) d\overline{x} \tag{33}$$

where σ_L is the standard deviation of the Gaussian random variable modeling lognormal shadowing in dB, μ_i depends on the distance attenuation law, $\mu_i = \ln(p_{t,i} \cdot k_p D_i^{-\alpha})$, and $h = \frac{10}{\ln(10)}$. In our analysis, σ_L is assumed to be the same for all signals.

An additional hurdle is present here, because of the integral in (33). We therefore propose an approximation to (33), exploiting the approach put forth by Holtzman in [26]. According to [26], given a function $\psi(\theta)$ of a Gaussian random variable θ with mean μ_θ and variance σ_θ^2, the expectation $\mathbb{E}[\psi(\theta)]$ can be approximated by

$$\mathbb{E}[\psi(\theta)] \approx \frac{2}{3}\psi(\mu_\theta) + \frac{1}{6}\psi\left(\mu_\theta + \sqrt{3}\sigma_\theta\right) + \frac{1}{6}\psi\left(\mu_\theta - \sqrt{3}\sigma_\theta\right). \tag{34}$$

For the examined case, it is observed that the change of variable

$$y = h \cdot \ln(\overline{x}) \tag{35}$$

that is, $\overline{x} = \exp\left(\frac{y}{h}\right)$, leads to rewrite (33) in the form

$$f_i(x_i) = \int_{-\infty}^{+\infty} \frac{1}{\exp\left(\frac{y}{h}\right)} \exp\left(\frac{-x_i}{\exp\left(\frac{y}{h}\right)}\right) \frac{1}{\sqrt{2\pi}\sigma_L} \times \exp\left(-\frac{(y-\mu_i)^2}{2\sigma_L^2}\right) dy \tag{36}$$

that can therefore be approximated as:

$$f_i(x_i) \approx \sum_{k=1}^{3} \frac{a_k}{b_{i,k}} \exp\left(\frac{-x_i}{b_{i,k}}\right) \tag{37}$$

where $a_1 = \frac{2}{3}$, $a_2 = a_3 = \frac{1}{6}$, $b_{i,1} = \exp\left(\frac{\mu_i}{h}\right)$, $b_{i,2} = \exp\left(\frac{(\mu_i + \sqrt{3}\sigma_L)}{h}\right)$ and $b_{i,3} = \exp\left(\frac{(\mu_i - \sqrt{3}\sigma_L)}{h}\right)$.

This linear combination of exponential functions allows to leverage the results obtained in the previous case of Rayleigh fading.

Hence, when lognormal shadowing is added, for n superimposed signals $P_{out}^{(1)}$ is approximated by

$$P_{out}^{(1)} \approx 1 - \sum_{k_1=1}^{3} a_{k_1} \cdot \ldots \cdot \sum_{k_{n-1}=1}^{3} a_{k_{n-1}} \sum_{k_n=1}^{3} a_{k_n}$$

$$P_{out}^{(j)} \approx \begin{cases} 1 - \prod_{h=1}^{j} \left(\sum_{k=h}^{n} \frac{\exp\left(\frac{-\hat{\gamma}_h \sigma^2}{\overline{X}_k}\right)}{\prod_{\substack{i=h \\ i \neq k}}^{n} \left(1 + \frac{\overline{X}_i}{\overline{X}_k} \hat{\gamma}_h\right)} \right) & j < n \\ 1 - \prod_{h=1}^{n} \left(\sum_{k=h}^{n} \frac{\exp\left(\frac{-\hat{\gamma}_h \sigma^2}{\overline{X}_k}\right)}{\prod_{\substack{i=h \\ i \neq k}}^{n} \left(1 + \frac{\overline{X}_i}{\overline{X}_k} \hat{\gamma}_h\right)} \right) \cdot \exp\left(-\frac{\hat{\gamma}_n \sigma^2}{\overline{X}_n}\right) & j = n \end{cases} \tag{32}$$

$$\times \left[\sum_{i=1}^{n} \frac{\exp\left(\frac{-\hat{\gamma}_1 \sigma^2}{b_{i,k_i}}\right)}{\prod_{\substack{j=1 \\ j\neq i}}^{n} \left(1 + \frac{b_{j,k_j}}{b_{i,k_i}} \hat{\gamma}_1\right)} \right] \tag{38}$$

and $P_{out}^{(j)}, j \geq 2$, follows from (28) and it is approximated by (39), as shown at the bottom of the page.

In next Section, the excellent accuracy of the approximations in (32), (38) and (39) will be demonstrated for several choices of system parameters.

IV. NUMERICAL RESULTS

An exemplary set of numerical results is reported next, in order to highlight the accuracy of the proposed analytical approaches, as well as to provide useful insights on the uplink performance of power-domain NOMA, when the dynamic-ordered SIC receiver is employed.

The results have been obtained for the following configuration: in (6), the target data rate $\hat{R}_{(j)}$ is set to 1.2 bits/s/Hz, $\forall j$, $j = 1, 2, \ldots, n$; in (30), the k_p constant is $\left(\frac{c}{4\pi f_c}\right)$, where c is the speed of light and omnidirectional antennas are assumed. The operating frequency is $f_c = 2$ GHz, the pathloss exponent is $\alpha = 2$ and the cell radius is $R = 1000$ m. As regards lognormal shadowing, unless otherwise stated, in (33) $\sigma_L = 4$ dB. To improve the base station capability to recover the signals coming from distinct UEs, the transmitted powers are set so as to attribute higher power levels to UEs closer to the base station. Unless otherwise stated, the UEs location along the cell radius is the one illustrated in Fig. 1. Namely, the ratio between the transmitted powers of UE_i and UE_j, with distances D_i and D_j from the base, $D_i < D_j$, is set to

$$\frac{p_{t,i}}{p_{t,j}} = 10^{\frac{(j-i)\Delta}{10}}, \tag{40}$$

and the power back-off step is $\Delta = 6$ dB.

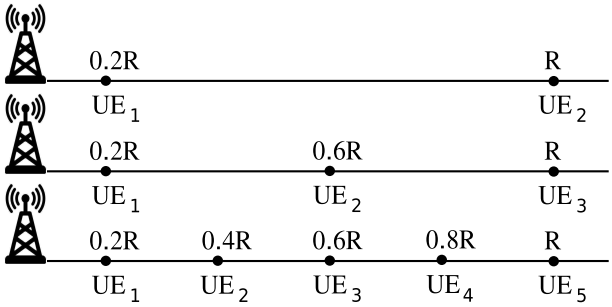

FIGURE 1. Users location along the cell radius when $n = 2, 3, 5$.

In the first set of figures, the outage probabilities are reported as a function of the largest average received Signal-to-Noise Ratio (SNR). Recalling that the UEs are indexed so that $\overline{X}_1 > \overline{X}_2 > \cdots > \overline{X}_n$, it follows that SNR $= \overline{X}_1/\sigma^2$. In other words, as the power law assignment privileges users that are closer to the base, the SNR is the average received signal-to-noise ratio of the UE that is the nearest to the base station.

When Rayleigh fading is considered, Fig. 2 shows $P_{out}^{(1)}$ as a function of the SNR, if $n = 2, 3, 5$ users are simultaneously transmitting. As indicated in Fig. 2, when $n = 2$, the distance D_1 of UE_1 from the base is $0.2R$ and the distance D_2 of UE_2 from it is R; when $n = 3$, $D_1 = 0.2R$, $D_2 = 0.6R$ and $D_3 = R$; when $n = 5$, $D_1 = 0.2R$, $D_2 = 0.4R$, $D_3 = 0.6R$, $D_4 = 0.8R$ and $D_5 = R$. Solid lines refer to the exact analytical evaluation, markers to $P_{out}^{(1)}$ values determined through Monte Carlo simulation, considering 10^5 samples for each plotted value. The perfect match between the analytical and the simulation results confirms the correctness of the exact closed-form of $P_{out}^{(1)}$ provided by (31). The figure also indicates that $P_{out}^{(1)}$ is close to 1 when the SNR is smaller than 5 dB, regardless of n. As a matter of fact, in this low SNR region, the achievable data rate of the strongest user is limited by the weak level of the received signal, rather than by the presence

$$P_{out}^{(j)} \approx \begin{cases} 1 - \prod_{h=1}^{j} \left(\sum_{k_h=1}^{3} a_{k_h} \cdot \ldots \cdot \sum_{k_{n-1}=1}^{3} a_{k_{n-1}} \sum_{k_n=1}^{3} a_{k_n} \cdot \left(\sum_{i=h}^{n} \frac{\exp\left(\frac{-\hat{\gamma}_h \sigma^2}{b_{i,k_i}}\right)}{\prod_{\substack{j=h \\ j\neq i}}^{n} \left(1 + \frac{b_{j,k_j}}{b_{i,k_i}} \hat{\gamma}_{h+1}\right)} \right) \right) & j < n \\ 1 - \prod_{h=1}^{n} \left(\sum_{k_h=1}^{3} a_{k_h} \cdot \ldots \cdot \sum_{k_{n-1}=1}^{3} a_{k_{n-1}} \sum_{k_n=1}^{3} a_{k_n} \cdot \left(\sum_{i=h}^{n} \frac{\exp\left(\frac{-\hat{\gamma}_h \sigma^2}{b_{i,k_i}}\right)}{\prod_{\substack{j=h \\ j\neq i}}^{n} \left(1 + \frac{b_{j,k_j}}{b_{i,k_i}} \hat{\gamma}_h\right)} \right) \right) \cdot \sum_{k=1}^{3} a_k \exp\left(-\frac{\hat{\gamma}_n \sigma^2}{b_{i,k}}\right) & j = n \end{cases} \tag{39}$$

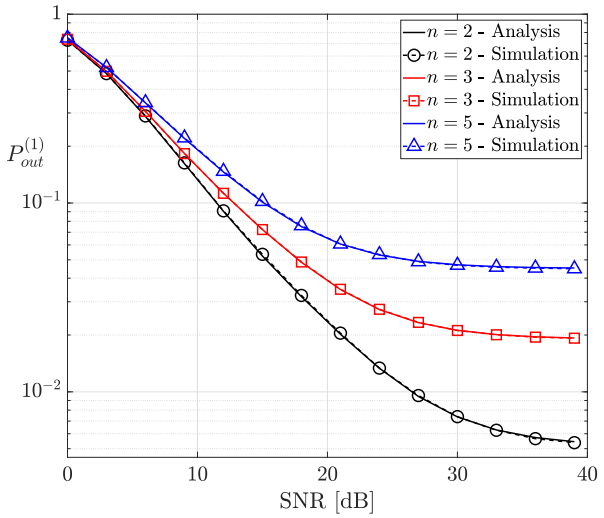

FIGURE 2. Rayleigh fading: $P_{out}^{(1)}$ as a function of the SNR, $n = 2, 3, 5$.

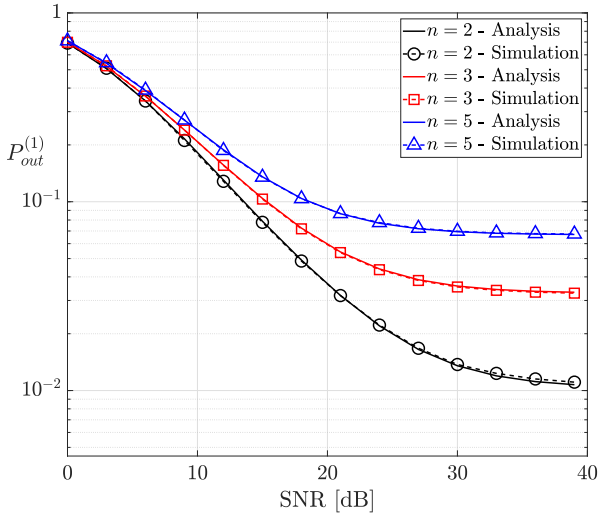

FIGURE 3. Rayleigh fading and log-normal shadowing: $P_{out}^{(1)}$ as a function of the SNR, $n = 2, 3, 5$.

of simultaneously transmitting users. As the SNR increases above 10 dB, the impact of a larger number of interfering users gradually becomes more evident. Yet, observe that for $n = 5$, $P_{out}^{(1)}$ is always below 1% for all SNR values in the $[15, +\infty]$ range.

Fig. 3 shows $P_{out}^{(1)}$ as a function of the SNR, when the received signal is subject to both Rayleigh fading and log-normal shadowing, and it reveals that the closed-form in (38) is an excellent approximation to the exact $P_{out}^{(1)}$ computed via simulation. In this scenario too, the impact on $P_{out}^{(1)}$ of a larger number of users can be appreciated only for SNR values greater than 10 dB. The relative position of the curves is the same as observed in Fig. 2. However, $P_{out}^{(1)}$ takes on higher values than in the presence of Rayleigh fading only. For instance, when SNR $= 30$ dB, for $n = 2$ $P_{out}^{(1)}$ increases from 7×10^{-3} determined in the presence of Rayleigh fading

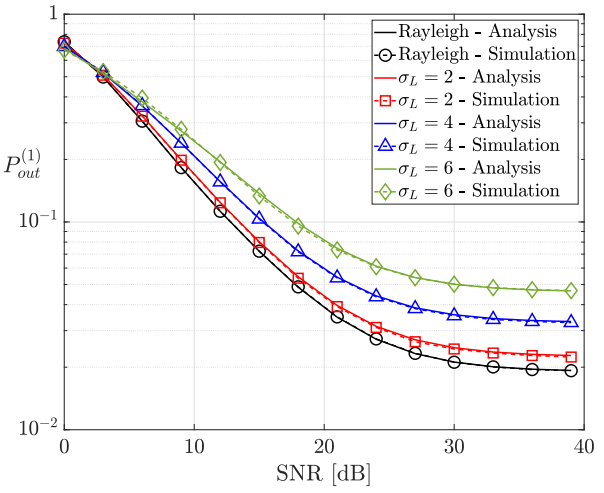

FIGURE 4. $P_{out}^{(1)}$, Rayleigh fading and Rayleigh plus lognormal, $n = 3$.

to 1.4×10^{-2} when lognormal shadowing is also taken into account, and raises from 4.7×10^{-2} to 6.9×10^{-2} for $n = 5$. This indicates that the shadowing plays a non-negligible role in the outage probability evaluation.

To better understand the influence of lognormal shadowing, Fig. 4 compares $P_{out}^{(1)}$ in the presence of Rayleigh fading against $P_{out}^{(1)}$ in the additional presence of lognormal shadowing, when $n = 3$ and three different values of σ_L, namely, 2, 4 and 6 dB are considered. The black lowest curve and the circle markers refer to the benchmark case of Rayleigh fading; the red, blue and green curves, paired with the square, triangle and diamond markers, respectively, refer to the Rayleigh plus lognormal case. The results corroborate what was previously anticipated, quantifying the remarkable impact of the shadowing on $P_{out}^{(1)}$ for increasing values of σ_L. For instance, when $\sigma_L = 6$ dB and SNR > 30 dB, $P_{out}^{(1)}$ is 2.4 times larger than for the case of Rayleigh fading only. Also note the tightness of the approximation provided by (38): here too, the results obtained by simulation are nearly undistinguishable from the analytical outcomes, no matter what σ_L value is examined.

Next, Fig. 5 and 5b report $P_{out}^{(1)}$, $P_{out}^{(2)}$ and $P_{out}^{(3)}$ for the case of Rayleigh fading and Rayleigh plus lognormal shadowing, respectively, when $n = 3$. As regards $P_{out}^{(2)}$ and $P_{out}^{(3)}$, these figure show the impressive accuracy of the approximation proposed in Section III and detailed in eqs. (32) and (39). Furthermore, they reveal that $P_{out}^{(2)}$ and $P_{out}^{(3)}$ take on significantly high values, with and without lognormal shadowing. As expected, $P_{out}^{(3)}$ takes on the worst values, as the signal coming from the third strongest user can be decoded only if both the second and the first strongest signals have already been decoded.

When considering both Rayleigh fading and lognormal shadowing, an alternative view is provided by Fig.6, that shows $P_{out}^{(1)}$, $P_{out}^{(2)}$ and $P_{out}^{(3)}$ as a function of D_2/R, the normalized distance of UE_2 from the base, when UE_1 and UE_3 distances are $D_1 = 0.2R$ and $D_3 = R$, respectively. This figure

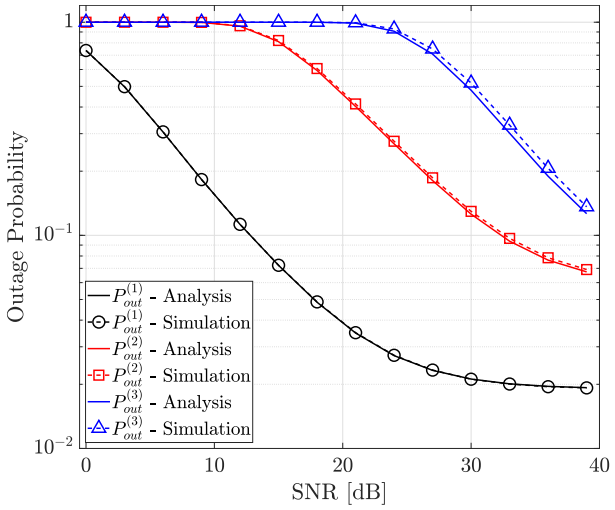

(a) Rayleigh Fading.

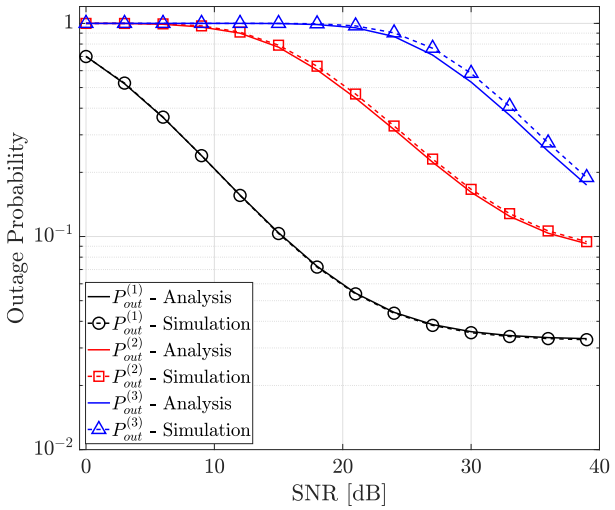

(b) Rayleigh fading plus log-normal shadowing.

FIGURE 5. Outage probability vs SNR, $n = 3$.

indicates that the values of $P_{out}^{(2)}$ and $P_{out}^{(3)}$ lie in the range of a few percentage points; equivalently stated, approximately in 90% of the cases it is possible to support 2 simultaneous communications (and in 80% of the cases even 3). If the involved UEs all require maximum reliability, this is unacceptable. Yet, resorting to power-domain NOMA becomes truly interesting in alternative settings: for instance, whenever communication redundancy can be introduced without an excessive overhead, as it happens when a modest number of packet re-transmissions are introduced and packets exhibit a modest size. The figure also shows that $P_{out}^{(2)}$ and $P_{out}^{(3)}$ minima lie at $D_2 = 0.4R$ and that they are not so critical, revealing that the location of the UEs does not have to be identified with extreme accuracy. Also observe that the tightness of the proposed approximation in evaluating $P_{out}^{(3)}$ slightly worsens as D_2 approaches D_3; this happens since the spacing δ_3 no longer verifies the assumption of taking on large values with probability close to 1.

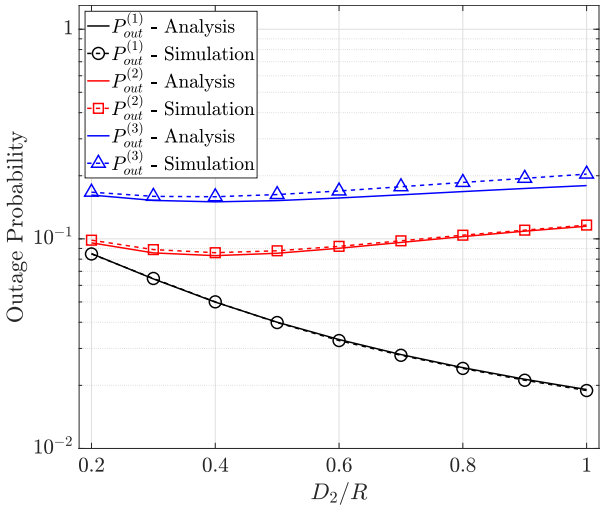

FIGURE 6. Outage probability as a function of D_2/R, $n = 3$, SNR = 30 dB.

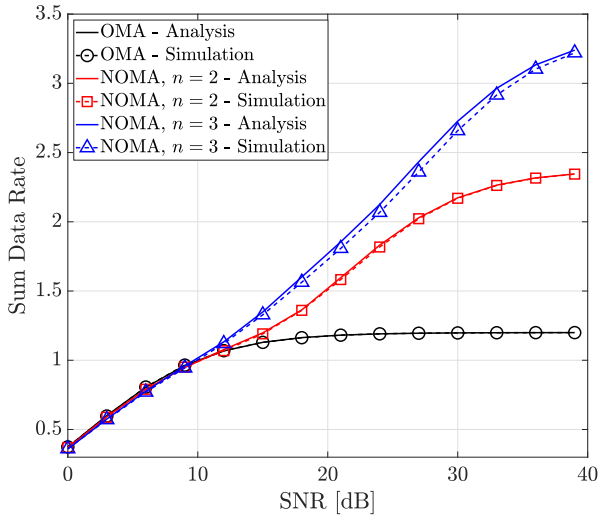

FIGURE 7. Sum data rate of OMA and NOMA as a function of SNR, Rayleigh and lognormal shadowing.

Last, Fig. 7 displays R_{NOMA}, the sum data rate of power-domain NOMA of (20), as a function of the SNR in the simultaneous presence of Rayleigh fading and lognormal shadowing, when $n = 2$ and $n = 3$, and compares it against the OMA data rate. The latter scheme is examined under the hypothesis that the signal-to-noise ratio of the OMA user coincides with SNR, the signal-to-noise ratio of the NOMA UE that is the nearest to the base station. Here too, the accuracy of the proposed approximation is striking. The gain of NOMA over OMA becomes more and more evident for increasing SNR values. Moreover, at high SNR regimes the NOMA system with $n = 3$ users achieves a sum data rate significantly greater than 2.4 bits/s/Hz, the maximum data rate NOMA attains when $n = 2$.

V. CONCLUSION

This work has proposed a novel analytical approach to evaluate the outage probabilities of uplink power-domain NOMA, when a dynamic-ordered SIC receiver is employed.

The method has been employed in the presence of Rayleigh fading, and Rayleigh plus lognormal shadowing. In the former setting, it has allowed to determine the probability that NOMA fails through an exact analytical expression, for a generic number of superimposed signals; in the second examined scenario, such probability has been obtained in closed-form via an excellent approximation. Moreover, the current study has put forth an approximated expression of the probability that the SIC receiver does not succeed in decoding the second, third, n-th strongest user. Monte Carlo simulations have demonstrated the accuracy of the results obtained through the proposed approximations, that clearly quantify the effects of an increasing number of simultaneous users on system performance. The analysis has also disclosed to what extent lognormal shadowing affects NOMA behavior, revealing that its presence significantly deteriorates performance with respect to the case of Rayleigh fading only.

APPENDIX A
DERIVATION OF $P_{out}^{(1)}$ FOR AN ARBITRARY NUMBER OF USERS

In the presence of Rayleigh fading, the outage probability $P_{out}^{(1)}$ is evaluated beginning with the special case $n = 2$. From (19), $P_{out}^{(1)}$ specializes to

$$P_{out}^{(1)} = 1 - (I_{S_1} + I_{S_2}) \tag{41}$$

where $S_1 = \{1, 2\}$, $S_2 = \{2, 1\}$,

$$\begin{aligned} I_{S_1} &= \iint_{\mathcal{D}_1} f_1(x_{(1)}) f_2(x_{(2)}) dx_{(2)} dx_{(1)} \\ &= \iint_{\mathcal{D}_1} \frac{1}{\overline{X}_1} \exp\left(-\frac{x_{(1)}}{\overline{X}_1}\right) \cdot \frac{1}{\overline{X}_2} \exp\left(-\frac{x_{(2)}}{\overline{X}_2}\right) dx_{(2)} dx_{(1)} \end{aligned} \tag{42}$$

and $\mathcal{D}_1$ is

$$\mathcal{D}_1 = \begin{cases} X_{(1)} \geq \hat{\gamma}_1 \cdot \left(X_{(2)} + \sigma^2\right) \\ X_{(1)} \geq X_{(2)} \geq 0 \end{cases}. \tag{43}$$

When the target data rate of the strongest user $\hat{\gamma}_1$ is at least equal to 1 bit/s/Hz, solving the integral in (42) gives

$$I_{S_1} = \frac{\exp\left(\frac{-\hat{\gamma}_1 \sigma^2}{\overline{X}_1}\right)}{1 + \frac{\overline{X}_2}{\overline{X}_1} \hat{\gamma}_1}. \tag{44}$$

From (44), I_{S_2} is readily determined as

$$I_{S_2} = \frac{\exp\left(\frac{-\hat{\gamma}_1 \sigma^2}{\overline{X}_2}\right)}{1 + \frac{\overline{X}_1}{\overline{X}_2} \hat{\gamma}_1} \tag{45}$$

and $P_{out}^{(1)}$ follows:

$$P_{out}^{(1)} = 1 - \left(\frac{\exp\left(\frac{-\hat{\gamma}_1 \sigma^2}{\overline{X}_1}\right)}{1 + \frac{\overline{X}_2}{\overline{X}_1} \hat{\gamma}_1} + \frac{\exp\left(\frac{-\hat{\gamma}_1 \sigma^2}{\overline{X}_2}\right)}{1 + \frac{\overline{X}_1}{\overline{X}_2} \hat{\gamma}_1} \right). \tag{46}$$

When $n = 3$, $P_{out}^{(1)}$ exhibits 3! distinct contributions. The first of them, I_{S_1}, $S_1 = \{1, 2, 3\}$, is

$$I_{S_1} = \iiint_{\mathcal{D}_1} f_1(x_{(1)}) f_2(x_{(2)}) f_3(x_{(3)}) \, dx_{(3)} dx_{(2)} dx_{(1)} \tag{47}$$

where $\mathcal{D}_1$ is identified by the conditions

$$\mathcal{D}_1 = \begin{cases} X_{(1)} \geq \hat{\gamma}_1 \cdot \left(X_{(2)} + X_{(3)} + \sigma^2\right) \\ X_{(1)} \geq X_{(2)} \geq X_{(3)} \geq 0. \end{cases} \tag{48}$$

So,

$$\begin{aligned} I_{S_1} &= \iiint_{\mathcal{D}_1} p_{123}(x_{(1)}, x_{(2)}, x_{(3)}) \, dx_{(3)} dx_{(2)} dx_{(1)} \\ &= \iiint_{\mathcal{D}_1} \frac{1}{\overline{X}_1} \exp\left(-\frac{x_{(1)}}{\overline{X}_1}\right) \cdot \frac{1}{\overline{X}_2} \exp\left(-\frac{x_{(2)}}{\overline{X}_2}\right) \\ &\quad \cdot \frac{1}{\overline{X}_3} \exp\left(-\frac{x_{(3)}}{\overline{X}_3}\right) \times dx_{(3)} dx_{(2)} dx_{(1)}. \end{aligned} \tag{49}$$

After a few lengthy steps, last integral is solved and leads to the following result

$$I_{S_1} = \frac{\exp\left(\frac{-\hat{\gamma}_1 \sigma^2}{\overline{X}_1}\right) \overline{X}_1^2 \overline{X}_2}{(\overline{X}_1 + \overline{X}_2 \hat{\gamma}_1)(\overline{X}_1 \overline{X}_2 + \overline{X}_1 \overline{X}_3 \hat{\gamma}_1 + \overline{X}_2 \overline{X}_3 \hat{\gamma}_1 + \overline{X}_2 \overline{X}_3 \hat{\gamma}_1^2)} \tag{50}$$

that more aptly is written as

$$I_{S_1} = \frac{\exp\left(\frac{-\hat{\gamma}_1 \sigma^2}{\overline{X}_1}\right)}{(1 + \frac{\overline{X}_2}{\overline{X}_1} \hat{\gamma}_1)(1 + \frac{\overline{X}_3}{\overline{X}_2} \hat{\gamma}_1 + \frac{\overline{X}_3}{\overline{X}_1} \hat{\gamma}_1 (\hat{\gamma}_1 + 1))}. \tag{51}$$

Once I_{S_1} is determined, all the remaining contributions can be obtained permuting over $\mathcal{S}_{\mathcal{N}}$. On purpose, the set $S_2 = \{1, 3.2\}$ is considered next, which provides the result

$$I_{S_2} = \frac{\exp\left(\frac{-\hat{\gamma}_1 \sigma^2}{\overline{X}_1}\right) \overline{X}_1^2 \overline{X}_3}{(\overline{X}_1 + \overline{X}_3 \cdot \hat{\gamma}_1)(\overline{X}_1 \overline{X}_2 + \overline{X}_1 (\overline{X}_3 + 2 \overline{X}_2 \overline{X}_3 \hat{\gamma}_1))}. \tag{52}$$

Observe that, when the sum $I_{S_1} + I_{S_2}$ is computed, it gives

$$\begin{aligned} C_1 &= I_{S_1} + I_{S_2} \\ &= \frac{\exp\left(\frac{-\hat{\gamma}_1 \sigma^2}{\overline{X}_1}\right) \overline{X}_1^2}{(\overline{X}_1 + \overline{X}_2 \hat{\gamma}_1)(\overline{X}_1 + \overline{X}_3 \hat{\gamma}_1)} = \frac{\exp\left(\frac{-\hat{\gamma}_1 \sigma^2}{\overline{X}_1}\right)}{(1 + \frac{\overline{X}_2}{\overline{X}_1} \hat{\gamma}_1)(1 + \frac{\overline{X}_3}{\overline{X}_1} \hat{\gamma}_1)}. \end{aligned} \tag{53}$$

If we now introduce the sets $S_3 = \{2, 1, 3\}$ and $S_4 = \{3, 1, 2\}$, permuting $\overline{X}_1$,$\overline{X}_2$ and $\overline{X}_3$ in (51) I_{S_3} and I_{S_4} are also determined. Their sum gives

$$\begin{aligned} C_2 &= I_{S_3} + I_{S_4} \\ &= \frac{\exp\left(\frac{-\hat{\gamma}_1 \sigma^2}{\overline{X}_2}\right) \overline{X}_2^2}{(\overline{X}_2 + \overline{X}_1 \hat{\gamma}_1)(\overline{X}_2 + \overline{X}_3 \hat{\gamma}_1)} = \frac{\exp\left(\frac{-\hat{\gamma}_1 \sigma^2}{\overline{X}_2}\right)}{(1 + \frac{\overline{X}_1}{\overline{X}_2} \hat{\gamma}_1)(1 + \frac{\overline{X}_3}{\overline{X}_2} \hat{\gamma}_1)}. \end{aligned} \tag{54}$$

$$I_{S_1} = \exp\left(\frac{-\hat{\gamma}_1\sigma^2}{\overline{X}_1}\right) \times \frac{\overline{X}_1^3\overline{X}_2^2\overline{X}_3}{(\overline{X}_1+\overline{X}_2\hat{\gamma}_1)(\overline{X}_1\overline{X}_2+\overline{X}_1\overline{X}_3+2\overline{X}_2\overline{X}_3\hat{\gamma}_1)(\overline{X}_1\overline{X}_2\overline{X}_3+\overline{X}_1\overline{X}_2\overline{X}_4+3\overline{X}_2\overline{X}_3\overline{X}_4\hat{\gamma}_1)}. \tag{59}$$

The same applies to $S_5 = \{3, 2, 1\}$ and $S_6 = \{2, 3, 1\}$, whose sum C_3 is

$$C_3 = I_{S_5} + I_{S_6} = \frac{\exp\left(\frac{-\hat{\gamma}_1\sigma^2}{\overline{X}_3}\right)\overline{X}_3^2}{(\overline{X}_3+\overline{X}_1\hat{\gamma}_1)(\overline{X}_3+\overline{X}_2\hat{\gamma}_1)} = \frac{\exp\left(\frac{-\hat{\gamma}_1\sigma^2}{\overline{X}_3}\right)}{(1+\frac{\overline{X}_1}{\overline{X}_3}\hat{\gamma}_1)(1+\frac{\overline{X}_2}{\overline{X}_3}\hat{\gamma}_1)}. \tag{55}$$

Therefore, in the presence of $n = 3$ users and under the previous hypothesis $\hat{\gamma}_1 \geq 1$, $P_{out}^{(1)}$ is amenable to the writing

$$P_{out}^{(1)} = 1 - \sum_{S_i \in S_N} I_{S_i} = 1 - \sum_{k=1}^{3} C_k = \\ = 1 - \left(\frac{\exp\left(\frac{-\hat{\gamma}_1\sigma^2}{\overline{X}_1}\right)}{(1+\frac{\overline{X}_2}{\overline{X}_1}\hat{\gamma}_1)(1+\frac{\overline{X}_3}{\overline{X}_1}\hat{\gamma}_1)} + \frac{\exp\left(\frac{-\hat{\gamma}_1\sigma^2}{\overline{X}_2}\right)}{(1+\frac{\overline{X}_1}{\overline{X}_2}\hat{\gamma}_1)(1+\frac{\overline{X}_3}{\overline{X}_2}\hat{\gamma}_1)} \right. \\ \left. + \frac{\exp\left(\frac{-\hat{\gamma}_1\sigma^2}{\overline{X}_3}\right)}{(1+\frac{\overline{X}_1}{\overline{X}_3}\hat{\gamma}_1)(1+\frac{\overline{X}_2}{\overline{X}_3}\hat{\Gamma})} \right). \tag{56}$$

When the case $n = 4$ is examined, $4! = 24$ terms contribute to $P_{out}^{(1)}$; yet, it is sufficient to compute the term that corresponds to the $S_1 = \{1, 2, 3, 4\}$ set, that is expressed by

$$I_{S_1} = \iiiint_{\mathcal{D}_1} f_1(x_{(1)}) f_2(\quad x_{(2)}) f_3(x_{(3)}) f_4(x_{(4)}) \\ \times dx_{(4)} dx_{(3)} dx_{(2)} dx_{(1)} \tag{57}$$

$\mathcal{D}_1$ now being given by

$$\mathcal{D}_1 = \begin{cases} X_{(1)} \geq \hat{\gamma}_1 \cdot \left(X_{(2)} + X_{(3)} + X_{(4)} + \sigma^2\right) \\ X_{(1)} \geq X_{(2)} \geq X_{(3)} \geq X_{(4)} \geq 0 \end{cases}. \tag{58}$$

Here too, the assumption of exponential pdf allows to solve (57) in closed-form, resulting in (59), as shown at the top of the page.

At first sight, last expression might look unmanageable and hinder $P_{out}^{(1)}$ determination. Yet, in analogy with the previous $n = 3$ case, the contribution in (59) has to be grouped with other conveniently identified terms, namely, those that correspond to the sets $S_2 = \{1, 2, 4, 3\}$, $S_3 = \{1, 3, 2, 4\}$, $S_4 = \{1, 3, 4, 2\}$, $S_5 = \{1, 4, 2, 3\}$ and $S_6 = \{1, 4, 3, 2\}$, leading to the partial sum

$$C_1 = \sum_{i=1}^{6} S_i = \frac{\exp\left(-\frac{\hat{\gamma}_1\sigma^2}{\overline{X}_1}\right)}{(1+\frac{\overline{X}_2}{\overline{X}_1}\hat{\gamma}_1)(1+\frac{\overline{X}_3}{\overline{X}_1}\hat{\gamma}_1)(1+\frac{\overline{X}_4}{\overline{X}_1}\hat{\gamma}_1)}. \tag{60}$$

In an analogous manner, 3 more partial sums are computed, so that altogether 4 terms are identified, $C_k, k = 1, 2, 3, 4$, the generic C_k being

$$C_k = \frac{\exp\left(-\frac{\hat{\gamma}_1\sigma^2}{\overline{X}_k}\right)}{\prod_{\substack{i=1 \\ i\neq k}}^{4}\left(1+\frac{\overline{X}_i}{\overline{X}_k}\hat{\Gamma}\right)} \tag{61}$$

and $P_{out}^{(1)}$ is then computed as

$$P_{out}^{(1)} = 1 - \sum_{k=1}^{4} C_k. \tag{62}$$

For an arbitrary number n of superimposed signals, n partial sums, each with $(n-1)!$ elements, have to be determined. By induction, the generic sum C_k turns out to be

$$C_k = \frac{\exp\left(-\frac{\hat{\gamma}_1\sigma^2}{\overline{X}_k}\right)}{\prod_{\substack{i=1 \\ i\neq k}}^{n}(1+\frac{\overline{X}_i}{\overline{X}_k}\cdot\hat{\gamma}_1)}, \tag{63}$$

so that $P_{out}^{(1)}$, the probability that power-domain NOMA cannot guarantee the target data rate to the strongest user, is finally written as

$$P_{out}^{(1)} = 1 - \sum_{k=1}^{n} C_k = 1 - \sum_{k=1}^{n} \frac{\exp\left(\frac{-\hat{\gamma}_1\sigma^2}{\overline{X}_k}\right)}{\prod_{\substack{i=1 \\ i\neq k}}^{n}\left(1+\frac{\overline{X}_i}{\overline{X}_k}\hat{\gamma}_1\right)}. \tag{64}$$

under the condition $\hat{\gamma}_1 \geq 1$ bits/s/Hz.

REFERENCES

[1] Cisco. *Cisco Annual Internet Report (2018–2023) White Paper*. Accessed: Jun. 10, 2022. [Online]. Available: https://www.cisco.com/c/en/us/solutions/collateral/executive-perspectives/annual-internet-report/white-paper-c11-741490.html
[2] N. Varsier, L.-A. Dufrene, M. Dumay, Q. Lampin, and J. Schwoerer, "A 5G new radio for balanced and mixed IoT use cases: Challenges and key enablers in FR1 band," *IEEE Commun. Mag.*, vol. 59, no. 4, pp. 82–87, Apr. 2021.
[3] Y. Liu, S. Zhang, X. Mu, Z. Ding, R. Schober, N. Al-Dhahir, E. Hossain, and X. Shen, "Evolution of NOMA toward next generation multiple access (NGMA) for 6G," *IEEE J. Sel. Areas Commun.*, vol. 40, no. 4, pp. 1037–1071, Apr. 2022.
[4] L. Dai, B. Wang, Y. Yuan, S. Han, I. Chih-Lin, and Z. Wang, "Non-orthogonal multiple access for 5G: Solutions, challenges, opportunities, and future research trends," *IEEE Commun. Mag.*, vol. 53, no. 9, pp. 74–81, Sep. 2015.
[5] S. M. R. Islam, N. Avazov, O. A. Dobre, and K.-S. Kwak, "Power-domain non-orthogonal multiple access (NOMA) in 5G systems: Potentials and challenges," *IEEE Commun. Surveys Tuts.*, vol. 19, no. 2, pp. 721–742, 2nd Quart., 2017.
[6] Z. Ding, X. Lei, G. K. Karagiannidis, R. Schober, J. Yuan, and V. Bhargava, "A survey on non-orthogonal multiple access for 5G networks: Research challenges and future trends," *IEEE J. Sel. Areas Commun.*, vol. 35, no. 10, pp. 2181–2195, Oct. 2017.

[7] B. Makki, K. Chitti, A. Behravan, and M.-S. Alouini, "A survey of NOMA: Current status and open research challenges," *IEEE Open J. Commun. Soc.*, vol. 1, pp. 179–189, 2020.
[8] K. Senel, H. V. Cheng, E. Björnson, and E. G. Larsson, "What role can NOMA play in massive MIMO?" *IEEE J. Sel. Topics Signal Process.*, vol. 13, no. 3, pp. 597–611, Jun. 2019.
[9] B. Clerckx, Y. Mao, R. Schober, E. Jorswieck, D. J. Love, J. Yuan, L. Hanzo, G. Y. Li, E. G. Larsson, and G. Caire, "Is NOMA efficient in multi-antenna networks? A critical look at next generation multiple access techniques," *IEEE Open J. Commun. Soc.*, vol. 2, pp. 1310–1343, 2021.
[10] G. Liu, Z. Wang, J. Hu, Z. Ding, and P. Fan, "Cooperative NOMA broadcasting/multicasting for low-latency and high-reliability 5G cellular V2X communications," *IEEE Internet Things J.*, vol. 6, no. 5, pp. 7828–7838, Oct. 2019.
[11] J.-B. Seo, B. C. Jung, and H. Jin, "Performance analysis of NOMA random access," *IEEE Commun. Lett.*, vol. 22, no. 11, pp. 2242–2245, Nov. 2018.
[12] H. Tabassum, E. Hossain, and M. J. Hossain, "Modeling and analysis of uplink non-orthogonal multiple access in large-scale cellular networks using Poisson cluster processes," *IEEE Trans. Commun.*, vol. 65, no. 8, pp. 3555–3570, Aug. 2017.
[13] M. Salehi, H. Tabassum, and E. Hossain, "Meta distribution of SIR in large-scale uplink and downlink NOMA networks," *IEEE Trans. Commun.*, vol. 67, no. 4, pp. 3009–3025, Apr. 2019.
[14] Z. Ding, R. Schober, and H. V. Poor, "Unveiling the importance of SIC in NOMA systems—Part 1: State of the art and recent findings," *IEEE Commun. Lett.*, vol. 24, no. 11, pp. 2373–2377, Nov. 2020.
[15] Z. Ding, R. Schober, and H. V. Poor, "Unveiling the importance of SIC in NOMA systems—Part II: New results and future directions," *IEEE Commun. Lett.*, vol. 24, no. 11, pp. 2378–2382, Nov. 2020.
[16] N. Zhang, J. Wang, G. Kang, and Y. Liu, "Uplink nonorthogonal multiple access in 5G systems," *IEEE Commun. Lett.*, vol. 20, no. 3, pp. 458–461, Mar. 2016.
[17] M. Al-Imari, P. Xiao, M. A. Imran, and R. Tafazolli, "Uplink non-orthogonal multiple access for 5G wireless networks," in *Proc. 11th Int. Symp. Wireless Commun. Syst. (ISWCS)*, Barcelona, Spain, Aug. 2014, pp. 781–785.
[18] Y. Liu, M. Derakhshani, and S. Lambotharan, "Outage analysis and power allocation in uplink non-orthogonal multiple access systems," *IEEE Commun. Lett.*, vol. 22, no. 2, pp. 336–339, Feb. 2018.
[19] Y. Gao, B. Xia, K. Xiao, Z. Chen, X. Li, and S. Zhang, "Theoretical analysis of the dynamic decode ordering SIC receiver for uplink NOMA systems," *IEEE Commun. Lett.*, vol. 21, no. 10, pp. 2246–2249, Oct. 2017.
[20] Y. Gao, B. Xia, Y. Liu, Y. Yao, K. Xiao, and G. Lu, "Analysis of the dynamic ordered decoding for uplink NOMA systems with imperfect CSI," *IEEE Trans. Veh. Technol.*, vol. 67, no. 7, pp. 6647–6651, Jul. 2018.
[21] M. Salehi and E. Hossain, "On coverage probability in uplink NOMA with instantaneous signal power-based user ranking," *IEEE Wireless Commun. Lett.*, vol. 8, no. 6, pp. 1683–1687, Dec. 2019.
[22] A. Agarwal, R. Chaurasiya, S. Rai, and A. K. Jagannatham, "Outage probability analysis for NOMA downlink and uplink communication systems with generalized fading channels," *IEEE Access*, vol. 8, pp. 220461–220481, 2020.
[23] A. Alqahtani, E. Alsusa, A. Al-Dweik, and M. Al-Jarrah, "Performance analysis for downlink NOMA over α-μ generalized fading channels," *IEEE Trans. Veh. Technol.*, vol. 70, no. 7, pp. 6814–6825, Jul. 2021.
[24] R. J. Vaughan and W. N. Venables, "Permanent expressions for order statistic densities," *J. Roy. Stat. Soc. B, Methodol.*, vol. 34, no. 2, pp. 308–310, Jan. 1972.
[25] M. G. Kendall and A. Stuart, *The Advanced Theory of Statistics*, vol. 1, 2nd ed. London, U.K.: Griffin, 1966.
[26] J. M. Holtzman, "A simple, accurate method to calculate spread-spectrum multiple-access error probabilities," *IEEE Trans. Commun.*, vol. 40, no. 3, pp. 461–464, Mar. 1992.

LUCA LUSVARGHI (Graduate Student Member, IEEE) received the master's degree *(summa cum laude)* in electronics engineering from the University of Modena and Reggio Emilia, Italy, in July 2019. He is currently pursuing the Ph.D. degree with the Department of Engineering "Enzo Ferrari," International ICT Doctorate School. His research interests include 5G and 6G technologies, particularly on cellular vehicle-to-everything (C-V2X) communications, and non-orthogonal multiple access (NOMA) techniques.

MARIA LUISA MERANI (Senior Member, IEEE) is currently with the Department of Engineering, University of Modena and Reggio Emilia, Italy, where she is also an Associate Professor. Her research interest includes the area of wireless networking. She served as the Technical Program Co-Chair for the Second IEEE International Symposium on Wireless Communication Systems 2005 (ISWCS'05), and IEEE Globecom, in 2007 and 2009 editions. In October 2009, she published her textbook *Hands On Networking: From Theory To Practice* (Cambridge University Press) and in the same year she was one of the authors of the book *Handbook of Peer-to-Peer Networking* (Springer). In 2010, she was the General Chair of the 15th edition of the IEEE International Symposium on Wireless Pervasive Computing. She served as the Editor of the IEEE TRANSACTIONS ON WIRELESS COMMUNICATIONS.